

## **CFD STUDY OF BLOOD FLOW IN A STENOSED HUMAN ARTERY**

**Thiago Felipe Calafati, calafati@ita.br<sup>1</sup>**  
**Claudia Regina de Andrade, claudia@ita.br<sup>1</sup>**  
**Edson Luiz Zaparoli, zaparoli@ita.br<sup>1</sup>**

<sup>1</sup>Instituto Tecnológico da Aeronáutica- ITA, Praça Marechal Eduardo Gomes, 50, Vila das Acácias, CEP 12228-900, São José dos Campos, SP

**Abstract:** *Blood flow numerical simulation has been undertaken to attain a better understanding of functional, diagnostic and therapeutic aspects of the blood flow. Blood can be considered as a pseudoplastic fluid with yield stress but many factors can influence blood viscosity and its behavior. The study of blood flow through stenosed human arteries is very important because of the fact that the cause and development of many arterial diseases leading to the malfunction of the cardiovascular system. At the present work, the blood flow in a stenosed artery is modeled applying the three-dimensional, unsteady, incompressible Navier-Stokes equations. The vessel wall is assumed rigid under a constant temperature and a uniform temperature is applied at the inlet boundary. The computational 3D domain is discretized using the finite volume method with an unstructured mesh. Numerical solution is obtained with an implicit transient scheme and the SIMPLE algorithm is employed for pressure velocity coupling. The influence of the Womersley number on the fluid flow patterns was studied and the reverse flow regions were also identified.*

**Keywords:** *CFD, stenosed blood flow, hemodynamic, non-Newtonian fluid, Womersley number, Casson's model*

### **1. INTRODUCTION**

Flow in arteries is the most common fluid dynamic phenomenon in biology. Fluids provide an indispensable medium for convection and diffusion of the numerous chemical and biochemical products required for the maintenance of biological function, and arteries provide the most efficient medium for the containment and transport of these fluids (Zamir, 2000). Blood flow in arteries is dominated by unsteady flow phenomena. The cardiovascular system is an internal flow loop with multiple branches in which a complex liquid circulates. Cessation or reduction in blood flow due to the presence of stenoses in the coronary arteries is the single largest cause of death in most nations (Chakravarty and Datta, 1988). Stenosed flow problem plays an important role to detection and quantification of stenosis serve as the basis for surgical intervention. Blood flow under normal physiologic conditions is an important field of study, as is blood flow under disease conditions. The majority of deaths in developed countries result from cardiovascular diseases, most of which are associated with some form of abnormal blood flow in arteries, (Ku, 1997). The simulation method can be useful for understanding the behavior properties of blood flow and rheological blood properties. Blood is a suspension of particles in an aqueous solution of constituents. The aqueous solution, called plasma, serves primarily as a transport vehicle for the various cells. The three most important in the human blood are the red blood cell, the white blood cells, and the blood platelets (Dinnar, 1981). The majority of the formed elements are red blood cells (RBCs) as a result they are important components in determining the flow characteristics of blood. At low shear rates, that is, values less than  $100 \text{ s}^{-1}$ , the RBCs aggregate and form rouleaux. Rouleaux aggregation disperses as the shear rate increases, reducing the viscosity of blood. The resulting shear-thinning behavior caused by rouleaux disaggregations in blood plasma is the principal cause of the non-Newtonian behavior of blood. However, with further increment of the shear rate beyond the low shear rate region, the shear-thinning characteristics disappear and blood demonstrates Newtonian behavior (Shewafraw et. al, 1995). (Sud and Sekhon, 1985) presented a mathematical model of flow in single arteries subject to pulsatile pressure gradient as well as the body acceleration. The results of their model have been used by them to further analyse the influence of body acceleration on arterial tree with 128 arteries. (Misra and Sahu, 1988) developed a mathematical model to study the flow of blood through large arteries under the action of periodic body acceleration.

Many of these studies were restricted to considering blood as a Newtonian fluid, although it is well known from a number of experimental observations that in most cases, blood behaves as a non-Newtonian fluid. Detection and quantification of the stenosis serve as the basis for surgical intervention. In the future, the study of arterial blood flow will lead to the prediction of individual hemodynamic flows in any patient, the development of diagnostic tools to quantify disease, and the design of devices that mimic or alter blood flow. (Ku, 1997).

At the present work, the transient laminar blood flow in a stenosed artery is studied taking account two different viscosity models (Power-Law and Casson) and comparing with Newtonian behavior for three different Womersley numbers: 4, 8 and 12. Results for the stream function and wall shear stress ( WSS ) are also presented to identify recirculation zones caused by the stenosis.

## 2. MATHEMATICAL FORMULATION

In this study we assume laminar incompressible flow, considering a straight axisymmetric artery with rigid walls, as depicted in Fig. (1).

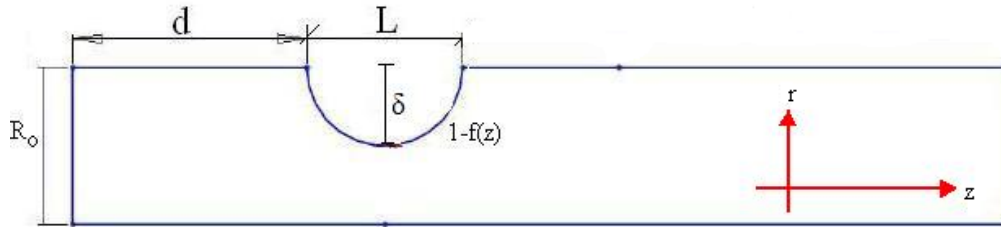


Figure 1. Schematic diagram of the stenosed artery.

Where:

$r$  = radial coordinate

$z$  = axial coordinate

$R_0$  = non-constricted artery radius

$R$  = artery radius throughout the constricted region

$L$  = stenosed segment length

$d$  = distance from the start of the arterial segment to the start of the stenosis

$\delta$  = height of the stenosis

The constricted region in Figure 1) of the artery domain is obtained using the following expressions:

$$\frac{R}{R_0} = \begin{cases} 1 - f(z) & \text{for } d \leq z \leq d + L \\ 1 & \text{otherwise} \end{cases} \quad (1)$$

In which  $f(z)$  is given by:

$$f(z) = A[l^{n-1}(z-d) - (z-d)^n], \text{ with } n = 2 \text{ and } A = \frac{\delta}{R_0^n} \frac{n}{n-1}$$

The tube length  $Z$  is equal a  $6 R_0$ . For artery stenosed, the internal surface dimensions are  $\delta = 5\text{mm}$ ,  $L = 10\text{mm}$ .

It is well know that blood behaves as a non-Newtonian fluid under certain flow conditions,(Tu and Devile, 1996). Two characteristic features emerge from experimental data: (i) the presence of a yield stress and (ii) the dependence of the viscosity with respect to shear rate. To take these effects into account, the governing equations (continuity and momentum) are stated as:

$$\nabla \cdot \vec{v} = 0 \quad (2)$$

$$\rho \left[ \frac{\partial \vec{v}}{\partial t} + (\vec{v} \cdot \nabla) \vec{v} \right] = -\nabla p + \nabla \cdot \tau \quad (3)$$

Where:

$\rho$  = blood density;  $\vec{v}$  = Velocity vector;  $p$  = Pressure field;  $t$  = time;  $\nabla(\cdot)$  = gradient operator;  $\nabla \cdot (\cdot)$  = divergent operator

$\tau$  = stress tensor expressed by:

$$\tau = \eta \gamma = \eta [\nabla \bar{v} + (\nabla \bar{v})^{tr}] \quad (4)$$

In Eq. 4 the superscript “tr” indicates the transpose;  $\eta$  is apparent viscosity of blood and  $\gamma$  is the shear rate. When the fluid is Newtonian, the stress tensor is proportional to the shear rate, and the constant of proportionality is called dynamic viscosity ( $\mu$ ). For Non-Newtonian fluids, the viscosity is called apparent viscosity ( $\eta$ ) that, herein, is expressed according to the chosen model see Eq. (6) and 7). (power law or Casson’s Model as presented in Fig.(2)

The non-linear partial differential equation system represented by Eq. 2 to 4 requires appropriate boundary conditions. At the present study, no-slip boundary conditions were imposed at rigid walls and the elasticity of the artery wall was dismissed. A null value to the pressure was specified at the artery outlet. At the inlet, a pulse axial velocity  $v_r(t)$  with time-varying function is imposed, as shown in Fig. (2).

$$v_r(t) = 3 + 3\sin(2\pi t/T) \quad (5)$$

Where:

T = period

t = time

For pulsatile flow, two dimensionless parameters are commonly used to characterize the flow conditions: (i) the Reynolds number  $R_e = \frac{\bar{\rho v}(2R)}{\mu}$ , where  $\rho$  is density of the fluid,  $\bar{v}$  is the characteristic velocity determined as the time-averaged mean velocity and  $\mu$  is dynamic viscosity and (ii) the Womersley number  $\alpha = R \left( \frac{\omega}{\nu} \right)^{0.5}$  with  $\omega = 2\pi/T$  is the frequency of the cyclic variation, R is the tube radius, and  $\nu$  is the kinematic viscosity.

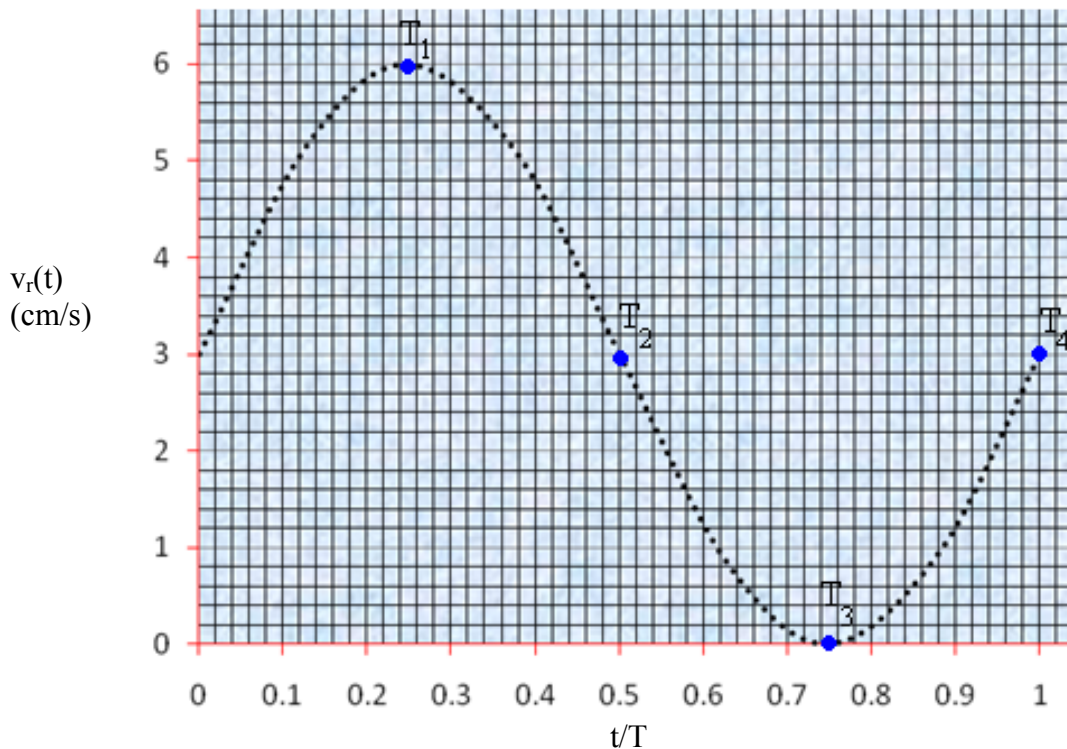


Figure 2. Inlet Pulse Velocity

While the Reynolds number is a comparison of the inertial force to viscous force, the number of Womersley can be interpreted as the ratio of the unsteady force to viscous force. In general, high Womersley number,  $Wo > 10$ , flows correspond to situations involving periods of rapid acceleration and deceleration. In Fig. (2)  $T_1$  indicates a peak flow time level,  $T_2$  is a time inside the decelerating phase,  $T_3$  corresponds to the zero net flow and  $T_4$ .  $T_2$  is a time inside the accelerating phase.

### 3. NON-NEWTONIAN BLOOD VISCOSITY MODEL

Diverse forms of constitutive equations have represented the shear-thinning behavior of blood. The most common constitutive equations characterizing this rheological behavior are divided into two categories namely Newtonian and non-Newtonian models. There are the variants of the non-Newtonian model characterizing shear-thinning behavior due to rouleaux dispersion at low shear rate. There is also the higher shear rate approximation single value viscosity, Newtonian model, which takes the shear independent constant viscosity of 0.0035 Pa.s at all shear rates.

#### 3.1. The Power-Law Model

The blood viscosity is modeled following the Power-law model (Cho and Kensey, 1991) and expressed as a function of the shear rate. The power law model for the blood viscosity takes form of

$$\eta = \eta_p = k\gamma^{n-1} \quad (6)$$

where  $k$ ,  $n$  are input parameters.  $k$  indicates a measure of the average fluid viscosity ( the consistency index );  $n$  is a measure of the deviation of the fluid from Newtonian model ( the power-law index). The index  $p$  is indicate for apparent viscosity. The value of  $n$  determines the class of the fluid:

- $n = 1$  Newtonian fluid
- $n > 1$  Shear-Thickening ( dilatants fluid )
- $n < 1$  shear-thinning ( pseudo-plastic)

#### 3.2 The Casson's Model

The Casson's model takes into account that blood at rest requires a minimum yield stress ( $\tau_0$ ) to start flowing. This behavior of blood and is given by the following equation:

$$\eta = \frac{\tau_0}{\gamma} + \frac{\sqrt{C\tau_0}}{\gamma} + C \quad (7)$$

where  $\eta$  is the viscosity of blood,  $\gamma$  is the shear stress,  $\tau_0$  yield stress and  $C$  is the Casson's rheological constant. The values of  $\tau_0$  and  $C$  depends on hematocrit  $H$ . Hematocrit is a percentage of whole blood occupied by cellular elements. So, the blood can be considered as pseudoplastic with yield stress. The blood behaves as Newtonian fluids for shear rate above  $200 \text{ s}^{-1}$  (Pedley, 1980; Berger and Jou, 2000), as shown in Fig. (3). The power law model adjust satisfactory at low shear rate values. The Casson's model shows a better agreement in comparison with experimental data, as presented in Figure (3).

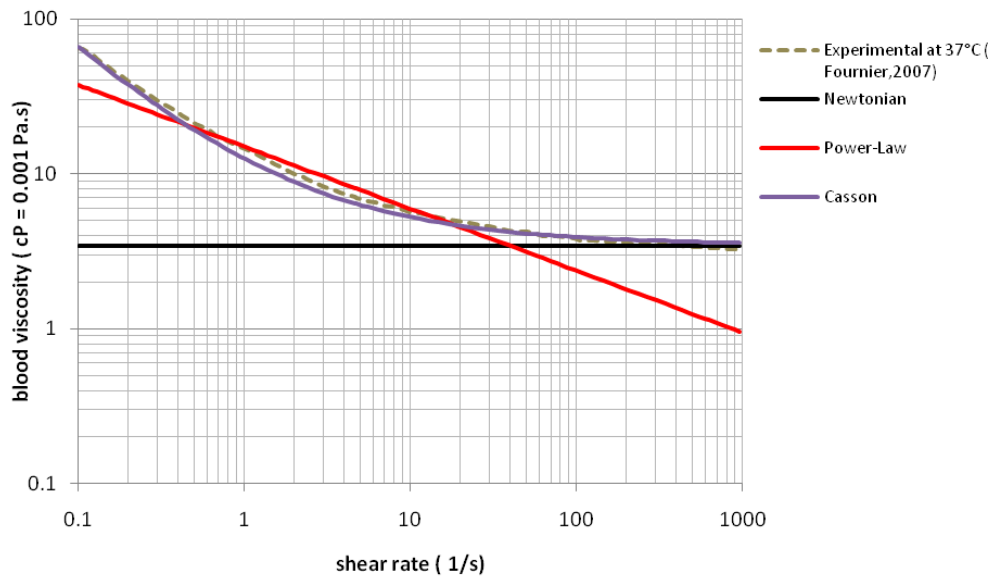


Figure 3. Blood viscosity model and experimental results.

#### 4. SOLUTION METHODOLOGY

The governing equations system ( Eq. 1 and Eq. 2 ) was discretized by the finite volume method employing a CFD package (Fluent 12.1.4 version). The pressure-velocity fields are coupled using the SIMPLE algorithm and the convective terms are treated by second order discretization. Two non-newtonian constitutive equations for the viscosity are tested and compared with the Newtonian model. The power-law constitutive relation is available in the CFD software but the Casson's model was implemented as a UDF C-language subroutine interpreted by the Fluent code. These main parameters are listed in Table (1).

Table 1. Viscosity models and the input parameters used in the simulations.

Models of blood viscosity	Parameters
Newtonian Model	$\rho = 1050 \text{ kg/m}^3$ ; $\mu = 0.00345 \text{ Pa.s}$
Power-Law Model	$k = 0.015 \text{ Pa}$ , $n = 0.6$ ; $\mu_\infty = 0.00345 \text{ Pa.s}$ ; $\mu_0 = 0.056 \text{ Pa.s}$ ; $\rho = 1050 \text{ kg/m}^3$
Casson's Model	$\tau_0 = 0.005 \text{ N}$ and $C = 0.0035 \text{ Pa.s}$

A computational mesh with quad elements was generated employing GAMBIT 2.4.6 software, as can be seen in Fig. (4). When the numerical residual reaches  $10^{-5}$ , the solution is considered as converged.

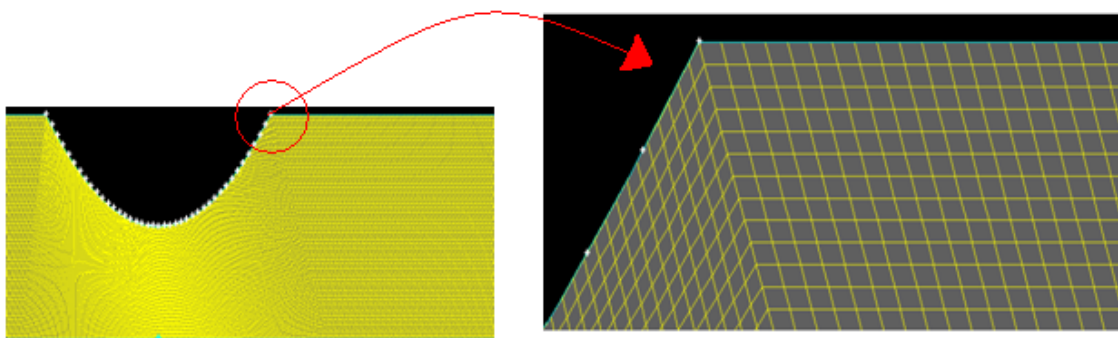


Figure 4. Mesh generated for the stenosed artery with a "zoom" region.

## 5. RESULTS

### 5.1. Validation procedure: steady-state blood flow inside a straight circular tube

Before simulating the stenosed artery configuration, a validation procedure was established by comparing numerical and analytical solution results for the blood flow inside a circular tube. These results are obtained for a power-law fluid flow under laminar steady-state fully developed conditions as provided in literature (Rohsenow et. al, 1998). The axial velocity component inside the tube is given by:

$$U = U_m \left( \frac{3n+1}{n+1} \right) \left[ 1 - \left( \frac{r}{R} \right)^{\frac{(n+1)}{n}} \right] \quad (8)$$

Where  $n$  is Power-law index

$R$ : is the radial coordinate

$U$ : velocity component at axial direction coordinate  $z$

$U_m$  : is the cross-section mean velocity

$R$ : is radius of the tube

The maximum velocity ( $U_{\max}$ ) is determined by the following equation:

$$U_{\max} = \left( \frac{\tau_w}{\mu_0} \right)^{\frac{1}{n}} \left( \frac{R}{1 + \frac{1}{n}} \right) \quad (9)$$

Where  $\tau_w$  is the Wall Shear Stress (WSS), defined as:

$$\tau_w = -\eta \frac{\partial u}{\partial n} \quad (10)$$

Where  $\eta$  is the apparent viscosity and  $(\partial u / \partial n)$  is the normal velocity gradient to the wall.

For the numerical solution, the tube length  $L$  is equal to  $20R$ . Figure 5 presents the numerical and analytical results for the power-law model with index  $n=0.3$ ;  $n=0.6$  and  $n=1$  (power law reduces to the Newtonian model). Note that the numerical solution captures the entry region which is longer as the  $n$  index increases. When  $n=1$ , the centerline axial velocity show that fully developed conditions are attained at  $z/D = 20$ . Otherhand, the Newtonian parabolic profile can be seen by analyzing the radial velocity component at the tube outlet ( $z/D = 20$ ), Fig. 6. As the  $n$  index value decreases, the radial velocity profile along the tube cross-section becomes flatter at  $r/R=0$ , and the maximum values also decay.



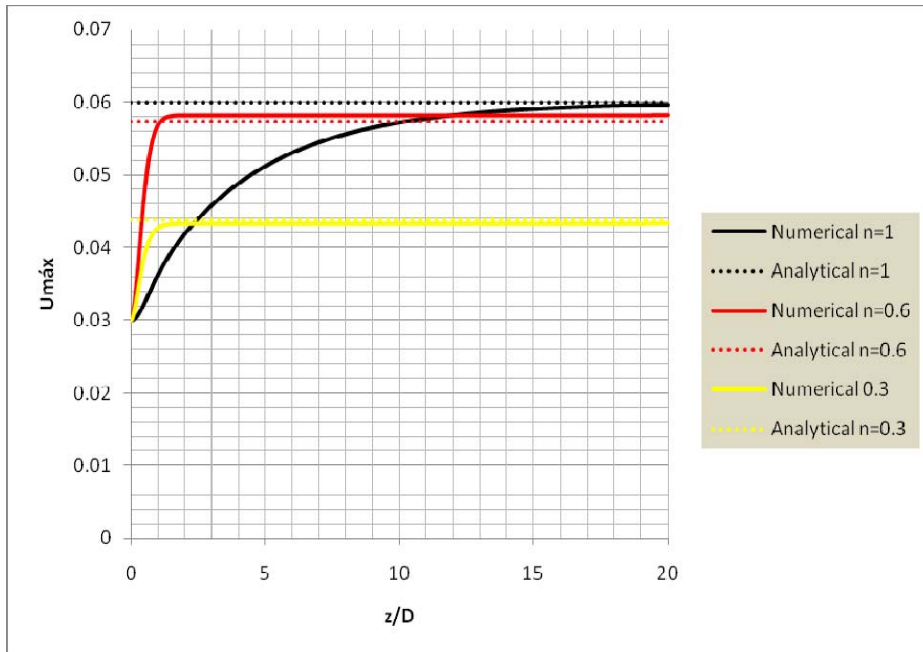


Figure 5. Axial centerline velocity profile along the tube axial direction

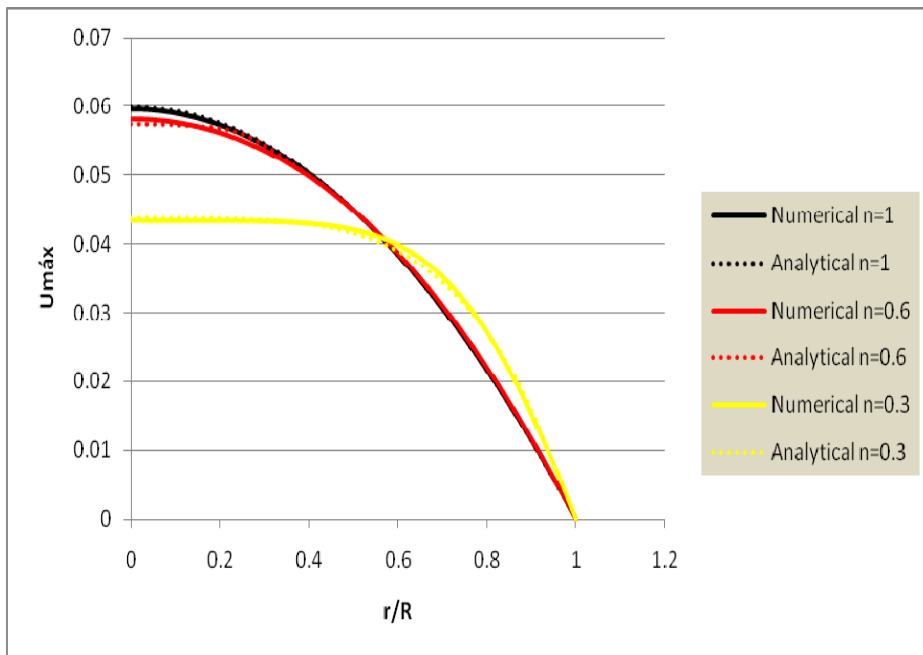


Figure 6. Radial velocity profile along the tube cross-section ( $r/R=20$ )

### 5.2 Stenosed artery

For the stenosed artery schematized in Fig. (1), the total length  $L$  is equal  $6R$ ,  $\delta = 5$  mm, resulting in a 50% stenosis condition. A laminar transient solution was obtained with the blood pulse velocity presented in Figure (2) for Reynolds number equal to 200 and three different Womersley numbers:  $Wo = 4, 8$  and  $12$ . Table (2) lists each timestep and period, respectively. Note that  $Wo = 4$  requires 1200 time steps to complete the sinusoidal pulse, as shown in Figure (6).

**Table 2. Parameters used in each simulation**

Womersley = 4	Womersley = 8	Womersley = 12
Time step 0.01 s	Time step 0.01 s	Time step 0.01 s
T=12 s	T=2.98 s	T=1.32 s

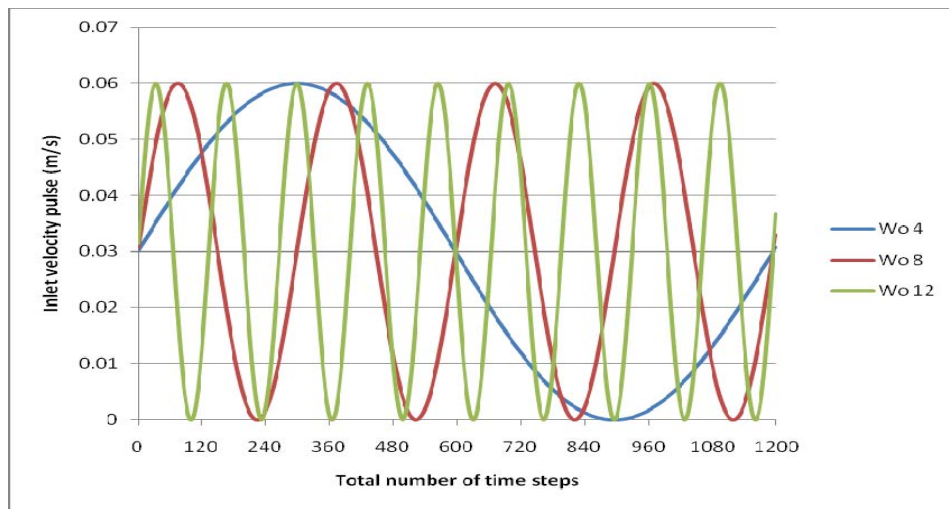


Figure 7. Inlet velocity pulse.

Two non-newtonian constitutive equations for the viscosity (Eq. 6 and Eq. 7) are tested and compared with the Newtonian model. The viscosity profile at the A-A' cross-section downstream the stenosis is presented in Fig. (8). The constant value corresponds to the Newtonian molecular viscosity. The power-law and Casson distributions present a similar behavior, except by the peak value immediately before the surface wall, which is shifted for the power-law in comparison with the Casson's model. It can be observed that along the A-A' cross-section, the Casson constitutive equation exhibits higher values than the two other formulations and agrees well with experimental data as earlier mentioned, Fig. (3).

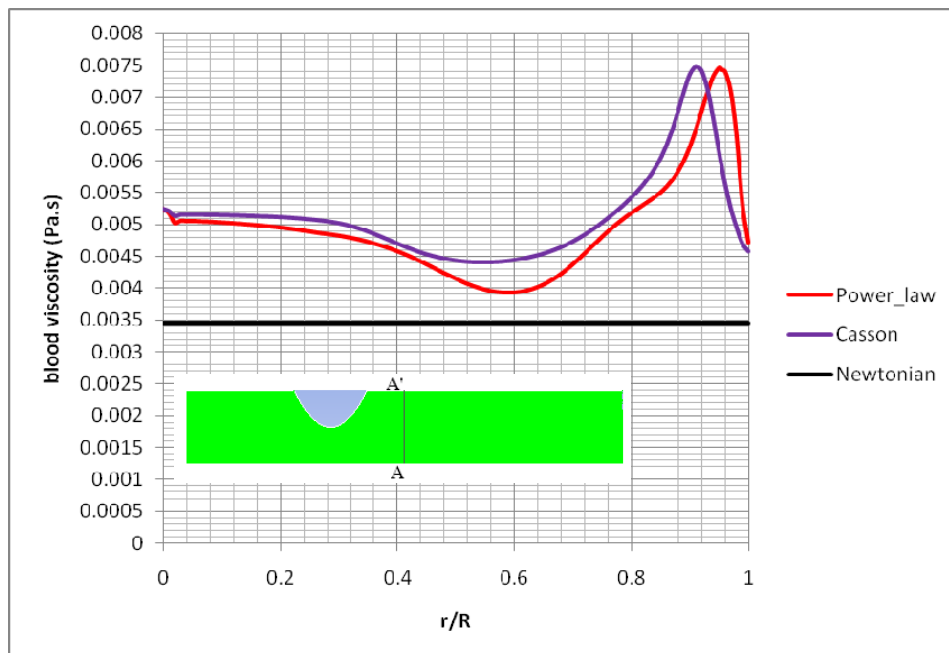


Figure 8. Viscosity distribution at a cross-section of the stenosed artery.

As mentioned in the literature (Aroesty and Gross, 1972), the Casson model is considered to be more accurate to capture the blood behavior. Based on this feature, the Womersley effect is shown only for the Casson's model. See Fig. (2) to identify the T1, T2, T3 and T4 time instants inside the velocity cycle. Figure (9) shows streamfunction distributions colored by velocity magnitude for  $Wo = 4$  at some time-instants of the velocity pulse: peak flow time (T1); decelerating phase (T2) zero net flow (T3) and accelerating phase (T4). It is observed that, as expected the minimum value occurs at Fig. (9c) when the fluid is at rest. As the flow is accelerated, a recirculation zone forms downstream the stenosis, Fig. (9d), which expands along the artery axial distance as the peak flow is reached, Figure (9a).



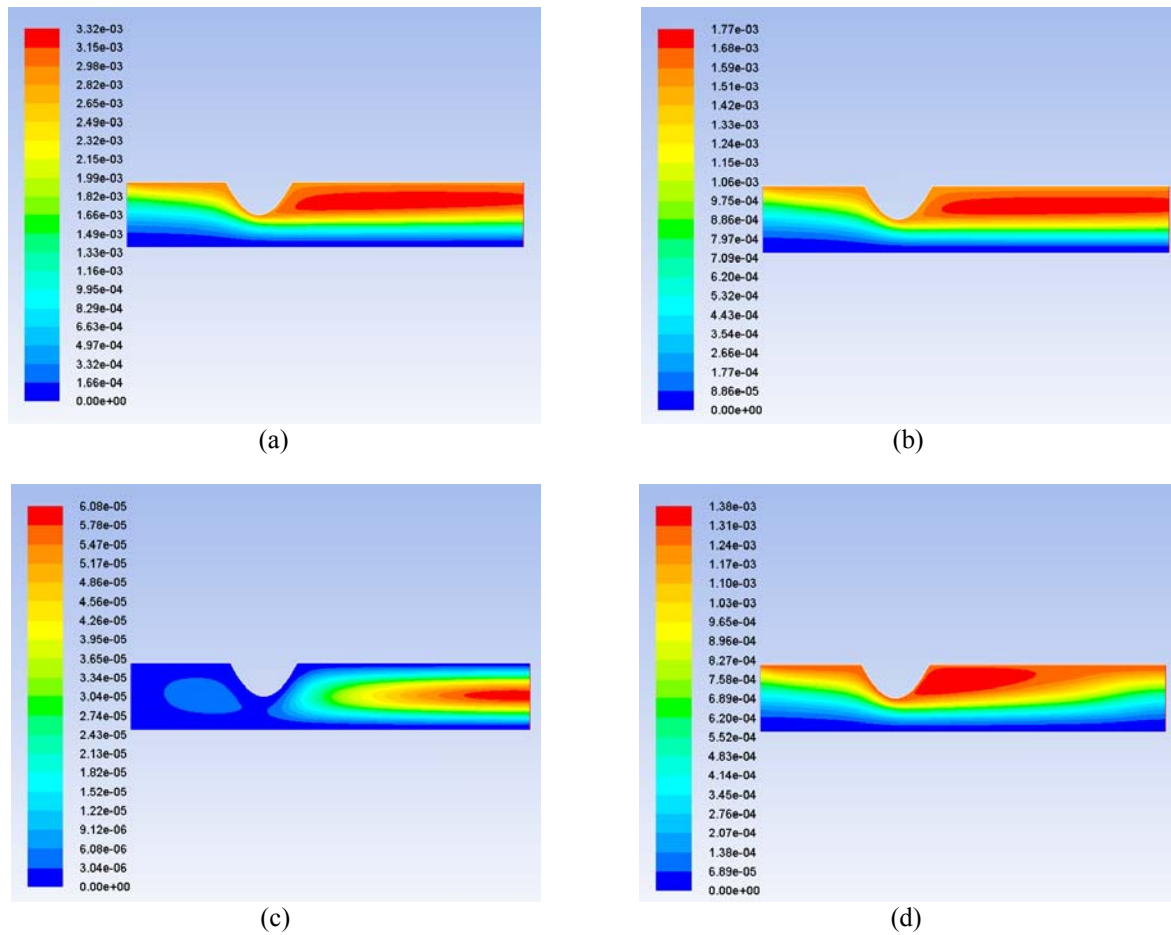


Figure 9. Casson's model: vortex development for Casson's model with  $Wo = 4$ : (a) peak flow time ( $T_1$ ) at  $t = 3$  s; (b) decelerating phase ( $T_2$ ) at  $t = 6$  s, (c) zero net flow ( $T_3$ ) at  $t = 9$  s and (d) accelerating phase ( $T_4$ ) at  $t = 11.7$  s.

Figure 10 presents the flow patterns for  $Wo = 8$  during the time-evolution. From Fig. (7) it can be seen that while  $Wo = 4$  presents only a peak flow, four maximum are observed for  $Wo = 8$  during the 12 s total time-period of simulation (1,200 timesteps). Note that during the decelerating phase, Fig. (10b), the streamfunction core is weaker, further downstream from the stenosis region.

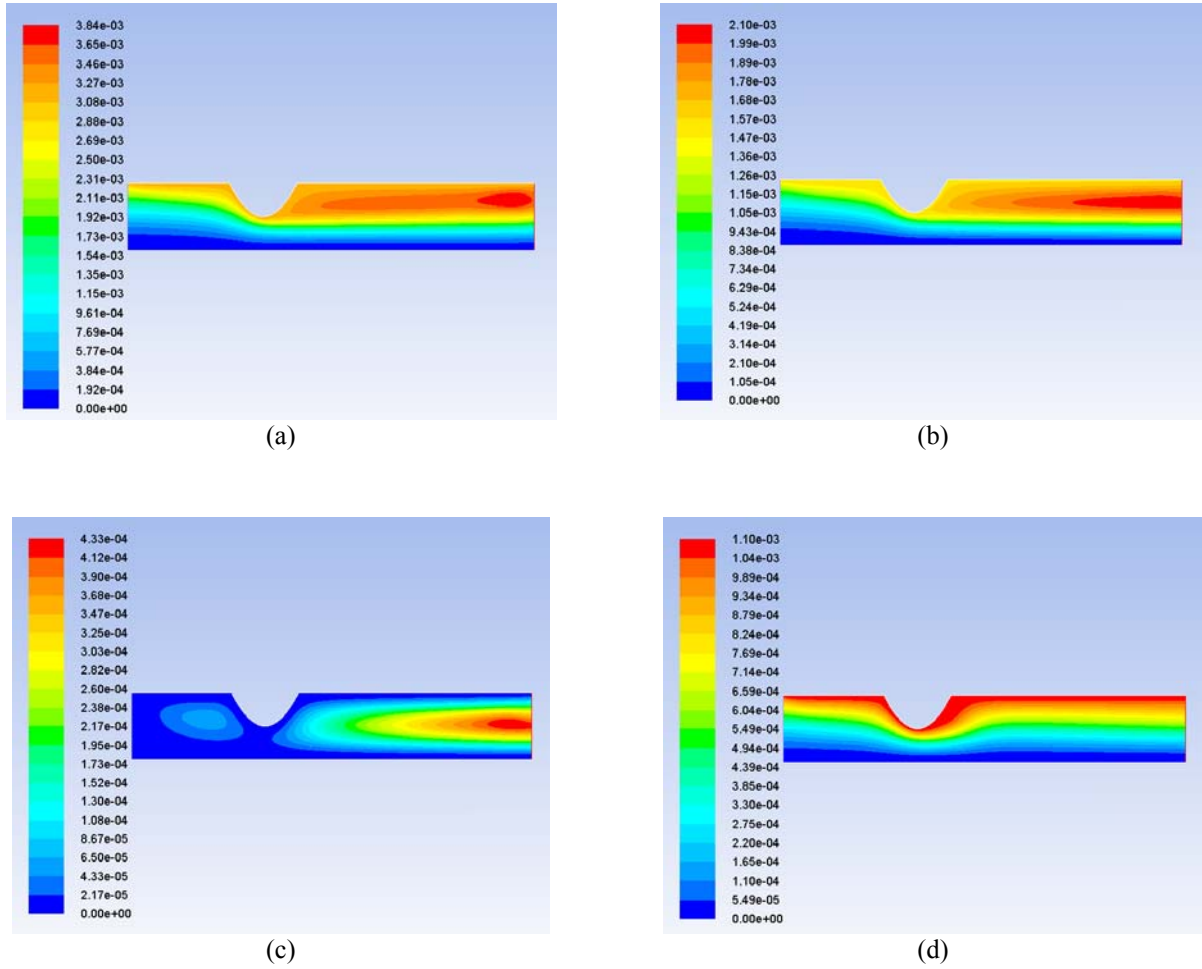


Figure 10. Casson's model: vortex development for Casson's model with  $Wo = 8$ : (a) peak flow time ( $T_1$ ) at  $t = 0.75$  s; (b) decelerating phase ( $T_2$ ) at  $t = 1.5$  s, (c) zero net flow ( $T_3$ ) at  $t = 2.25$  s and (d) accelerating phase ( $T_4$ ) at  $t = 3$  s.

As the Womersley number increases, Fig. (11), the pulsatile effect over the artery blood flow becomes more intense due to a reduction in the pulse period (or increase in its frequency, as shown in Fig. (7)). This fact leads to the encapsulating of the recirculation zone inhibiting the vortex displacement downstream of the stenosis, Fig. (11a).

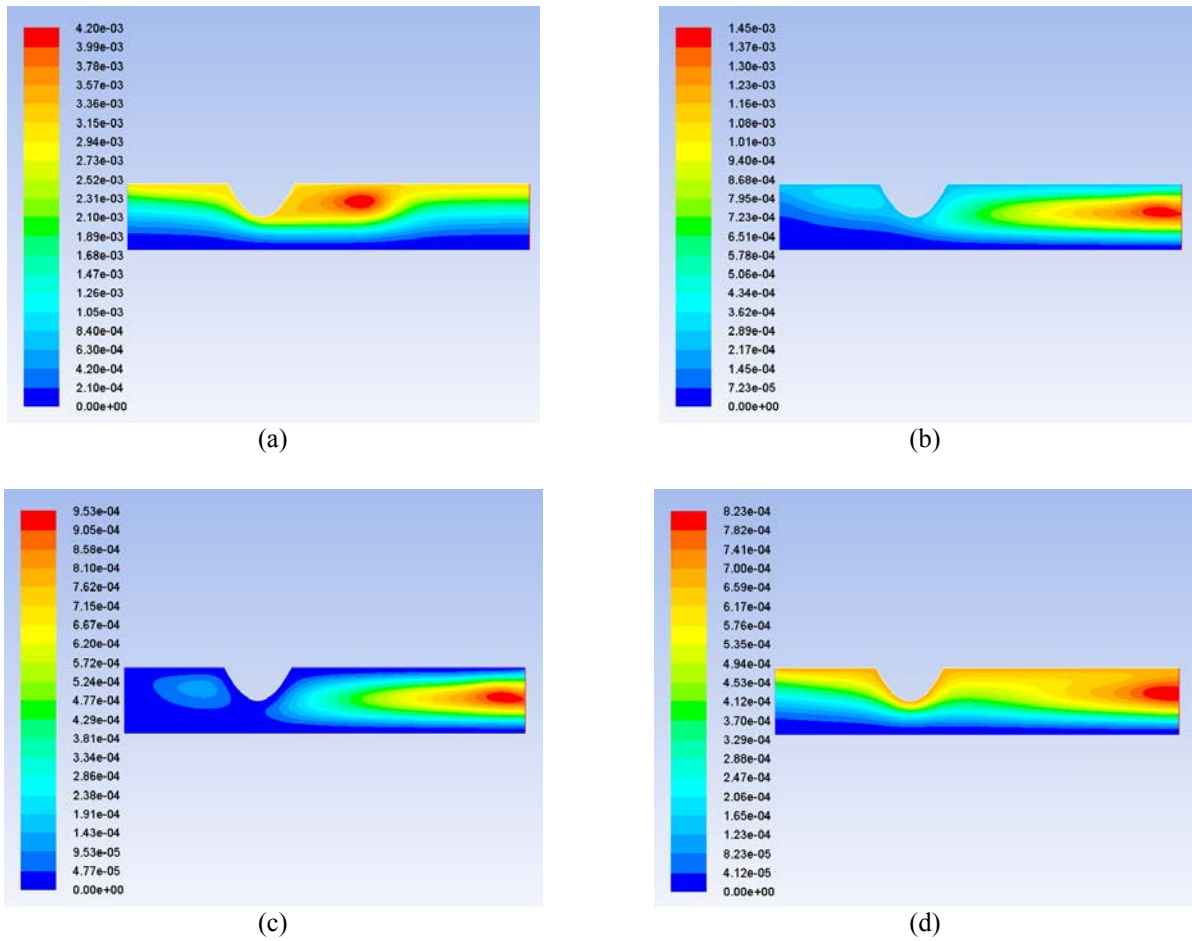


Figure 11. Casson's model: vortex development for Casson's model with  $Wo = 12$ : (a) peak flow time ( $T_1$ ) at  $t = 0.32$  s; (b) decelerating phase ( $T_2$ ) at  $t = 0.68$  s, (c) zero net flow ( $T_3$ ) at  $t = 1$  s and (d) accelerating phase ( $T_4$ ) at  $t = 1.29$  s

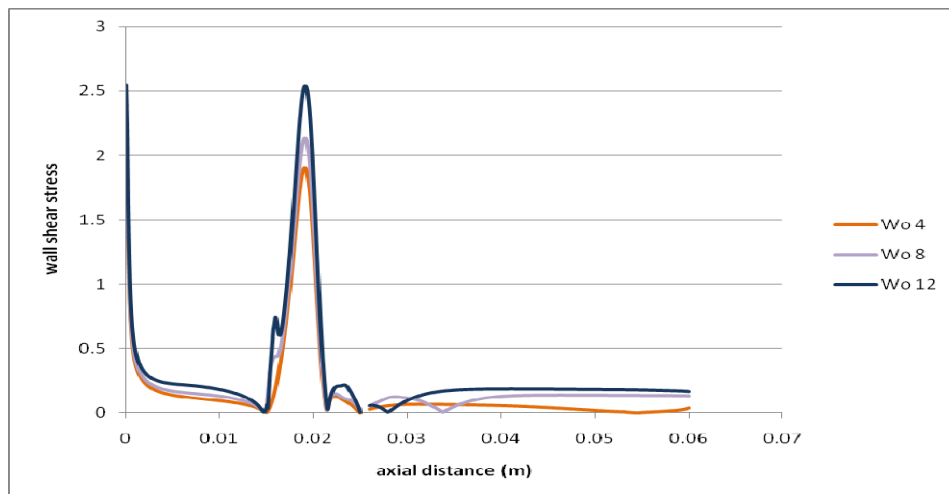


Figure 12. – Casson's model: Wall shear stress [Pa] at Womersley 4, 8 and 12

Figure 12 illustrates the wall shear stress (WSS) results, that is another parameter of physiological interest, obtained employing the Casson viscosity model. It can be noticed that the WSS peaks occur on the stenosis wall close to the occlusion vertex (minimum flow rate area due to the stenosis obstruction). All these three peaks are quite similar, increasing slightly with Womersley number.

## **6. FINAL REMARKS**

At this work, the blood flow in a stenosed artery is numerically simulated. Results showed that the Casson viscosity model is more suitable to capture the blood flow characteristics. The Womersley number ( $Wo$ ) influence on the velocity-streamfunction patterns was also investigated. It was observed that for higher  $Wo$  values, the pulsatile effect on the vortex development downstream the stenosis region becomes encapsulated around this region.

## **7. REFERENCES**

- Aroesty, J. and Gross, J., "Pulsatile Flow in Small Blood Vessels, *Biorheology*, 9, 1972, 33-43.
- Buchanan Jr J.R, Kleinstreuer C.,1998. "Simulation of particle-hemodynamics in a partially occluded artery segment with implications to the initiation of microemboli and secondary stenoses". *J Biomech Eng* 120:446±54.
- Buchanan, J.R, Kleinstreuer C.; Comer J.K. 2000."Rheological effects on pulsatile hemodynamics in a stenosed tube" *Computer & Fluids* 29. pp. 695-724
- Chakravarty, S., Datta, A. Mandal, P.K., 1996, "Effect of body acceleration on unsteady flow of blood past a time-dependent arterial stenosis, *Math. Comput*". *Model.* 24, 57-74.
- Chaturani, P. Palanisamy, V., 1991. "Pulsatile flow of blood with periodic body acceleration". *Int. J. Eng. Sci* 29, 113-121.
- Chaturani, P., Palanisamy, V., 1990."Casson fluid model of pulsatile flow of blood flow under periodic body acceleration", *Biorheol.* 27, 619-630.
- Dinnar, U.R.,(1981)."Cardiovascular Fluid Dynamics". CRC Press, Florida.
- Fournier, R.L., "Basic Transport Phenomena in Biomedical Engineering", 2<sup>nd</sup> ed, New York: Taylor & Francis Group, 2007
- Merrill EW. 1969. "The rheology of blood". *Physiol Rev*;26:863±88.
- Mirsa, J.C. Sahu, B.K., 1988."Flow through blood vessels under the action of a periodic acceleration field : A mathematical analysis", *Comput. Math. Appl.* 16 , 993-1016.
- Ojha M, Cobbold RSC, Johnston KW, Hummel RL. 1989. "Pulsatile flow through constricted tubes: an experimental investigation". *J Fluid Mech* 1989;203:123±97.
- Rohsenow, W.M., Hartnett, J.P. and Cho, Y. I.,1998, "Handbook of Heat Transfer". 3<sup>rd</sup>, McGraw Hill, USA.
- Sud, V.K. Sekhon, G.S., 1985. "Arterial flow under periodic body acceleration", *Bull. Math. Biol.* 47, 35-52.
- Sud, V.K., Sekhon, G.S.,1986. "Analysis of blood through a model of the human arterial system under periodic body acceleration", *J. Biomech.* 19 , 929-941.
- Tu, C., Deville, M., Dheur, L., and Vnderschuren, L. (1992) Finite-element simulation of pulsatile flow through arterial stenosis. *J. Biomechanics* 25, 1141-1152.
- Zamir, M., 2000. "The physics of pulsatile flow". Ed. Springer-Verlag, New York, Inc , 1-7.

## **8. RESPONSIBILITY NOTICE**

Authors are responsible for the material included in this paper.